SUPPLEMENT TO THE *WELDING JOURNAL*, JULY 2014
Sponsored by the American Welding Society and the Welding Research Council

Brazing of CMSX-4 with a Boron- and Silicon-Free Ni-Co-Zr-Hf-Cr-Ti-Al Brazing Alloy

Combining Hf and Zr as a melting point depressant improved ductility and reduced the brazing temperature to a range more compatible when joining superalloys

BY X. HUANG

ABSTRACT

In this study, a new boron- and silicon-free brazing alloy containing Ni-Co-Zr-Hf-Cr-Ti-Al was used to join CMSX-4 under three conditions. The resultant joint interface microstructure and hardness of the constituents were evaluated and are reported here. It was found that by using a combination of Hf and Zr as a primary melting point depressant, the amount of each element could be effectively reduced while still achieving a relatively low liquidus for the brazing alloy. The new brazing alloy is able to successfully join CMSX-4 with complete metallic bonding. Although two types of interfacial Zr-rich intermetallic compounds were observed after a 40-min brazing cycle, their hardness values are similar to that of a superalloy substrate. With the application of pressure during brazing or postbrazing homogenization heat treatment, the intermetallic compounds are substantially reduced. Furthermore, the formation of cellular γ/γ' in the interfacial region is discussed in this paper.

KEYWORDS

• Boron- and Silicon-Free Braze Alloy • CMSX-4 • Narrow Gap Brazing

Introduction

Joining or repair of superalloy gas turbine hot section components can be achieved using welding or brazing. For superalloys containing substantial gamma prime (γ') or gamma double prime (γ''), welding of these alloys can cause excessive cracking in the heat-affected zone and fusion zone in addition to distortion. Brazing, on the other hand, has advantages over welding in terms of its capability in joining hard-to-weld superalloys and reducing cost due to batch processing. During the brazing cycle, the brazing alloy melts, joins the superalloys, and solidifies during cooling or via an isothermal diffusion process. The bulk superalloys being joined stay in solid state during brazing such that brazing alloys must have a lower melting range/temperature than that of superalloys. Traditional nickel-based brazing alloys contain relatively large amounts of a melting point depressant (MPD) such as boron (B), silicon (Si), and phosphorus (P) to reduce the melting temperature of nickel, nickel-chromium, or cobalt matrix to suitable brazing temperature ranges between 1000° and 1250°C (Ref. 1). Furthermore, these MPD elements are also responsible for the wetting and flowing behavior of brazing alloys on the superalloy substrate during the brazing cycle. Boron, due to its high diffusivity, is preferred where homogeneous joint compositions are required.

However, the use of traditional B, Si, and/or P-containing brazing alloys can lead to the formation of brittle, hard phases (often containing Cr) within the joint and reductions of tensile, fatigue, and creep properties, in addition to compromised corrosion resistance due to chromium depletion. Brittle borides (or carboborides), in either discrete or eutectic form, formed during the brazing cycle have been observed to affect the mechanical properties of the joint, noticeably the ductility and fatigue life (Refs. 2–4). As shown in Fig. 1, the cycles to failure during low-cycle fatigue (LCF) tests of both wide-gap braze (WGB) and narrow-gap braze (NGB) joints are substantially reduced due to the presence of brittle, B-containing intermetallic compound(s). The ductility of NGB joint was also significantly lower than that of the base metal; crack initiation in NGB joint was found to be associated with intermetallic phases (Ref. 5). A process to improve the mechanical integrity of the braze joint/repaired area generally requires the use of a costly diffusion

X. HUANG (Xiao.huang@carleton.ca) *is with Dept. of Mechanical and Aerospace Engineering, Carleton University, Ottawa, Ont., Canada.*

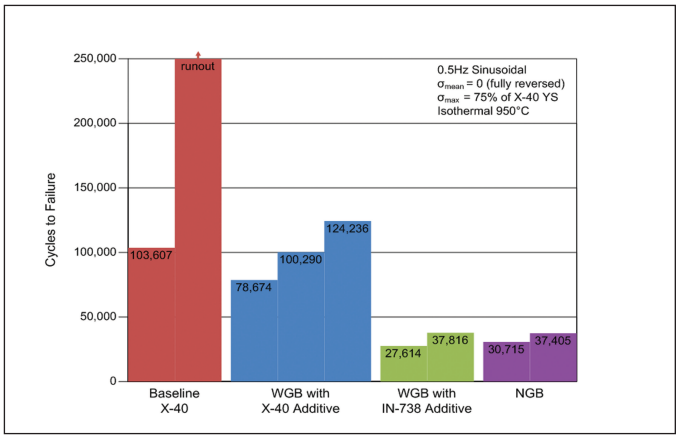

Fig. 1 — LCF property of NGB and WGB joints with B-containing brazing alloy in comparison to base metal X-40 (Ref. 4).

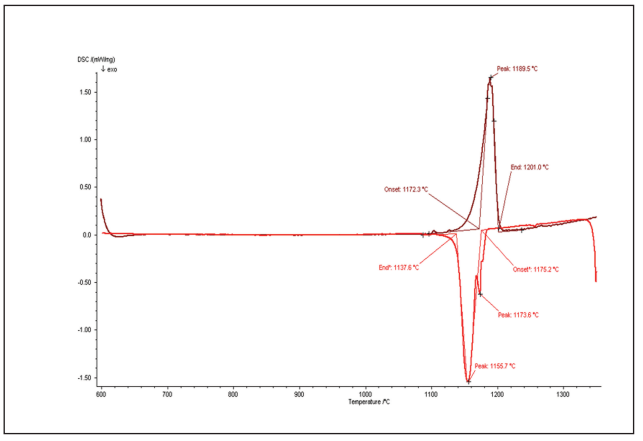

Fig. 2 — Heating (top) and cooling (bottom) heat flux curves for the braze alloy. A heating/cooling rate of 25°C/min was used.

Table 1 — Braze Alloy Composition and Melting Range

	Ni	Co	Zr	Hf	Cr	Ti	Al	Solidus °C	Liquidus °C
Development Alloy								1172.3 (heating)	1201 (heating)
Composition (BF-1)	Bal.	15	10	7.5	7.5	6.4	3.6	1137.6 (cooling)	1175.2 (cooling)
Actual Alloy Ingot (BF-1)	Bal.	13.52	9.07	7.2	6.94	6.9	3		

Table 2 — Composition of CMSX-4 (wt-%)

	Cr	Co	Al	Ti	W	Mo	Ta	Re	Hf	Zr	Ni
CMSC-4	6.4	9.6	5.6	1.0	6.4	0.6	6.5	2.9	0.1	–	Bal.

cycle. This approach may reduce the amount of brittle boride phases to a certain extent, but the properties of the superalloys may be affected adversely. Alternatively, the use of Ni-Cr-Hf or Ni-Cr-Zr brazing alloy has shown to alleviate some of the disadvantages associated with B- or Si-containing brazing alloys and provide improved high-temperature tensile properties (reaching 76% of the base metal's yield strength and 93% of the ductility [Refs. 6, 7]), as well as LCF and creep resistance. Close to 80% of the base metal's fatigue life and 90% of the rupture strength have been reported with the use of Ni-Cr-Zr brazing alloy (Refs. 6, 7).

The use of hafnium as a melting point depressant for a nickel-based brazing alloy provides a different approach to produce a ductile brazing alloy with moderate brazing temperatures at or below 1240°C.

Ductile braze alloys containing Ni-Hf-Cr, Ni-Hf-Co, and Ni-Hf-Mo were initially developed by Buschke and Lugscheider (Ref. 8) as alternatives to boron- and silicon-containing brazing alloys. While these alloys showed good ductility, they require relatively high brazing temperatures (1235°C) in order to produce good wetting. Some superalloys may suffer incipient melting at this temperature. Also, the joints with Ni-Hf-Cr showed galvanic corrosion when tested in an aqueous salt solution (Ref. 9). An alloy with the composition of Ni-18.6Co-4.5Cr-4.7W-25.6Hf was used to join superalloys at a brazing temperature of 1240°C (Ref. 10). The W in the brazing alloy was found to increase the melting temperature of the alloy.

Nickel-based boron-free brazing alloys containing either Hf or Zr, reported in the literature, have compositions of about 26–34 wt-% Hf or 11–19 or 40–60 wt-% Zr (Ref. 11). The intermetallic phases formed in the Ni-Zr eutectic alloys were found to be softer than borides, a good indication of reduced brittleness of the joint. However, the addition of Hf or Zr in some alloys was quite high, requiring long diffusion heat treatment (up to 36 hours) at high brazing temperatures (up to 1320°C) in order for the brazed joint to reach a composition similar to a superalloy substrate. With the addition of hafnium or zirconium alone in the nickel substrate, the lowest achievable melting temperatures are 1190° and 1170°C, respectively.

Another nonboron-containing nickel-based brazing alloy with manganese was developed for epitaxial brazing of single crystal superalloys (Refs. 12, 13). The alloy contains manganese in the range of 20–58 wt-%; in particular, Ni-(20–23)Ge alloys were developed for brazing single crystal superalloys. Ge is a melting point depressant that has also shown to assist the formation of γ/γ' in the brazement (Ref. 14). A hardness test showed the microhardness in the joint to be equivalent to that of the base metal (Ref. 15). However, being a substitutional element in the Ni the matrix, the diffusion time for the purpose of homogenizing the joint is quite lengthy (Ref. 16).

To develop new brazing alloy systems that are devoid of B or Si, the compositions of eutectic constituents in precipitation-hardened superalloys

Fig. 3 — Vacuum furnace brazing setup (samples were inside graphite holder and weights were applied in one trial).

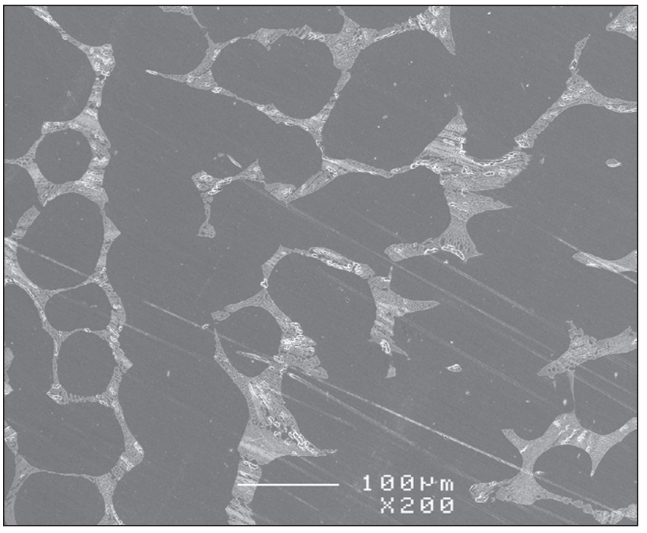

Fig. 4 — Ni-Co-Zr-Hf-Cr-Ti-Al braze alloy.

can serve as a reference point. A brazing alloy, Ni-10Co-8Cr-4W-13Zr, developed based on a eutectic composition, was used to successfully braze single-crystal superalloys at a brazing temperature of 1270°C (Ref. 17). It was reported that a eutectic Ni-based brazing alloy with a composition of 3.1–8.2% Co, 6.8–38.5%Cr, 0–12.6%Al, 0–11.5%Ti, 0–1.3%Mo, 0–23.1Ta, 0–2.4%W, 0-5.1%Nb, 0–1%Re, 0–0.4%Hf, and 0–0.6%Y had sufficient fluidity during brazing once the eutectic temperature T_E was reached (Ref. 18).

This research was initiated with the objective to develop a boron-free multi-element brazing alloy system that could be tailored to different substrate alloys and brazing temperature ranges while providing a joint composition similar to that of the superalloys. The selection of alloying elements and their percentages was based primarily on the following strategies: 1) eutectic composition(s) of binary Ni-M system (Ni-Hf, Ni-Zr, Ni-Al, and Ni-Ti); 2) elements that are present in current superalloy systems; and 3) compositions of eutectic phases found in superalloys.

In the system developed in this study, Hf and Zr were included, in a smaller percentage, in addition to other elements (Co, Cr, Ti, and Al) found in the eutectic phases. In a controlled-composition range, Zr can improve the ductility and stress rupture life of the brazed joint. Hf, on the other hand, has the ability to strengthen the γ′ phase in precipitation-hardened superalloys and improve the oxidation resistance and coatability of the brazed joints. A series of alloys containing Ni, Co, Zr, Hf, Cr, W, Ti, and Al was cast and the liquidus and solidus of the alloys were evaluated. Among these alloys, one of them (Table 1) exhibited the following melting and solidification characteristics (Fig. 2) and was used in this work to join CMSX-4, a second-generation, single-crystal superalloy.

CMSX-4 is a nickel-based single-crystal superalloy known for its high strength and creep resistance at very high temperature. It is commonly used in the gas turbine industry for turbine blades and vanes. The γ′solvus is greater than earlier generations of superalloys due to the removal of grain boundary strengtheners, and it is estimated to be as high as 1286°C (Ref. 19). As the alloy is exposed to severe operating conditions, there is always a need to repair gas turbine components in order to reduce the overall life cycle cost. When selecting repair and refurbishment technologies, it is to be realized that DS and SX high-strength superalloys are among the most difficult alloys for joining and repair. During repair, several operations, including machining, grinding, and heat treatment, are known to cause recrystallization (Ref. 20) and formation of cellular γ/γ′ (Ref. 21). The formation of cellular γ/γ′ microstructure in the alloy has been observed to reduce the fatigue strength of CMSX-4 (Ref. 22). Reported in this reference, the fatigue cracks were found to be predominantly initiated from the cellular area and arrested at the interface between the cellular and unaffected regions. One of the reasons for such reduction in fatigue strength is believed to be the lack of grain boundary strengthening elements (B, Zr, and Hf) in SX alloys (Ref. 21). In one particular study, a boron-containing coating (called a "damage cure" coating) was used to supply grain boundary strengthener to a heavily worked and heat treated CMSX-10 containing localized cellular γ/γ′and the result was a substantial

Table 3 — Summary of Sample Processing Conditions

Sample No.	Condition
NGB1	1240°C for 40 min
NGB2	1240°C for 40 min with pressure 50 lb/in.^{2}
NGB3	1240°C for 40 min + 1200°C for 10 h for homogenization

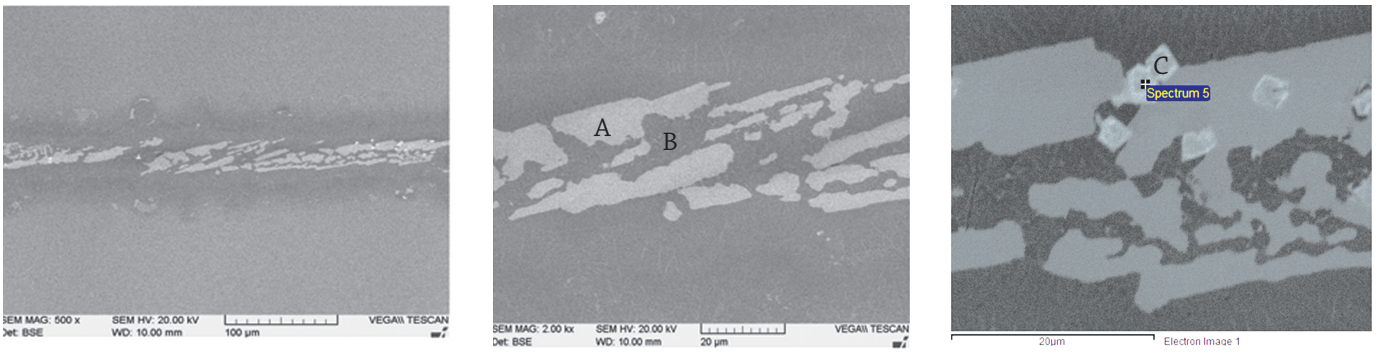

Fig. 5 — SEM images before etching (NGB1)with different phases labeled A, B and C..

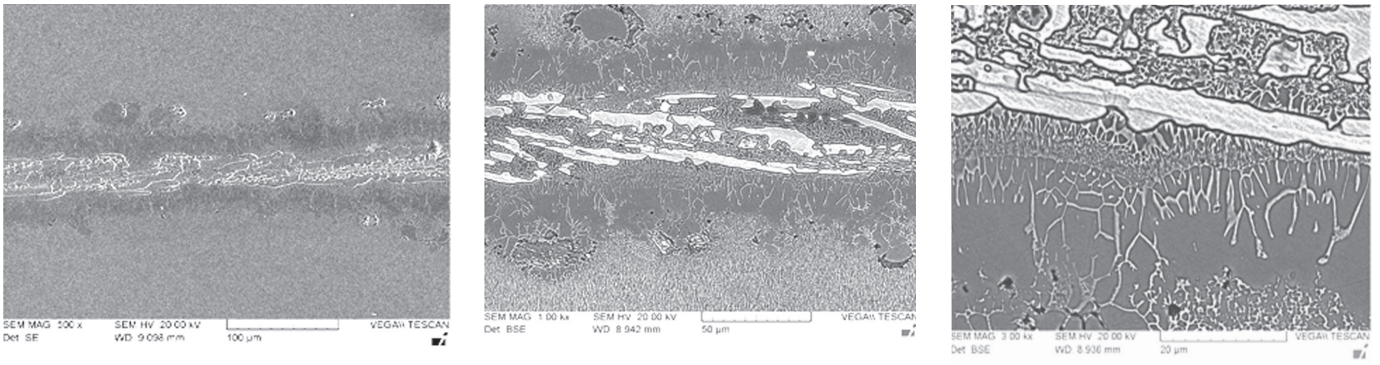

Fig. 6 — SEM images of NGB1 interface in the etched condition.

Table 4 — EDS Results of Phases in NGB1

Element	Concentration, at.-%		
	White Phase (A) in Fig. 5B	Gray Matrix (B) in Fig. 5B	Cubic-Shaped Phase (C) in Fig 5C
Al	8.88	12.44	5.53
Ti	2.42	4.19	4.63
Cr	5.54	10.76	6.50
Co	11.03	11.62	7.85
Ni	62.75	58.95	43.13
Zr	7.17	1.44	17.09
Hf	2.21	0.00	8.32
W	0.00	0.60	2.58
Re	0.00	0.00	6.95

increase in fatigue life. The addition of grain boundary strengthener relocated the fatigue initiation site from cellular site to internal casting defects. This further supports the beneficial effects of using a brazing alloy containing grain boundary strengtheners such as Zr and Hf as included in the brazing alloy developed in this study.

Materials and Experimental Procedures

CMSX-4 bars were purchased from Alcoa Howmet Research Center (Michigan). The 0.625-in.- (1.6-cm-) diameter bars, with <001> direction along the longitudinal direction of the bar, were supplied in the solution-treated condition (usually takes place at temperatures between 1277° and 1318°C (Ref. 19)). One of the boron- and silicon-free brazing alloys was cast by Sophisticated Alloys, Inc., (Pa.). The actual brazing alloy composition is provided in Table 2.

Foils were fabricated from the cast brazing alloy bar (0.75 cm diameter) to a thickness of 250 μm. Base material sample buttons (1.6 cm diameter) were sectioned from the CMSX-4 bar after the secondary orientation was marked. After gentle polishing of one side of the CMSX button surfaces to 600-grit finishing, the samples were cleaned and assembled into a graphite sample holder with braze alloy foil sandwiched in between. The two CMSX-4 buttons were aligned in the sample holder to maintain the secondary orientation. The samples inside the graphite jig were placed into a vacuum furnace as shown in Fig. 3. Three different vacuum brazing cycles were conducted under the conditions detailed in Table 3. The peak temperature was determined to be below the solution heat treatment temperature for CMSX (1277°C) and to reduce the likelihood of recrystalization, which occurs at temperatures above 1240°C (Refs. 23, 24). For the initial brazing, the following cycle parameters were used:

- Evacuate the furnace for 2 h and purge with Ar. Evacuate again to 10^{-5} torr before turning heating elements on.
- Heat from room temperature to 1080°C at 10°C/min.
- Hold at 1080°C for ½ h.
- Heat to 1240°C at 25°C/min.
- Hold at 1240°C for 40 min.
- Furnace cool to room temperature.

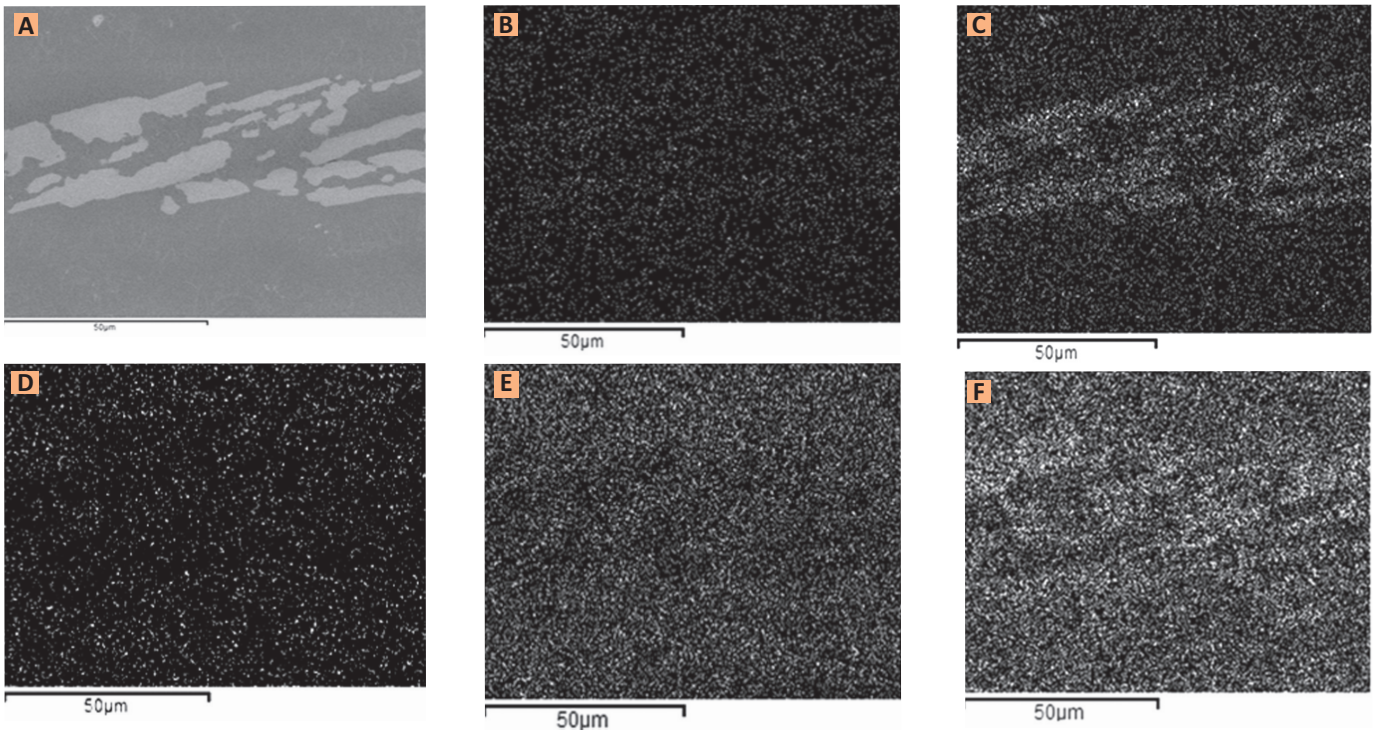

Fig. 7 — Elemental maps of the NGB1 interface. A — BSE SEM image; B — Hf; C — Zr; D — Al; E — Ti; F — Cr.

After brazing, samples were sectioned, ground, and polished. The microstructure of the brazed samples was first observed in the as-polished condition using backscatter electron (BSE) microscopy. The percentages of key alloying elements in the brazed region of three samples were measured by energy-dispersive spectrometry (EDS). After EDS analysis, the samples were electrolytically etched in a solution of 35.6 mL H_2SO_4, 37.5 mL HNO_3, and 9.4 mL H_3PO_4 at 7 V for 120 s. The microstructural analysis was performed using a TESCAN scanning electron microscope (SEM). Lastly, the microhardness values of various phases were measured using a Vickers hardness tester (Clemex Technologies Inc., Longueuil, QC, Canada).

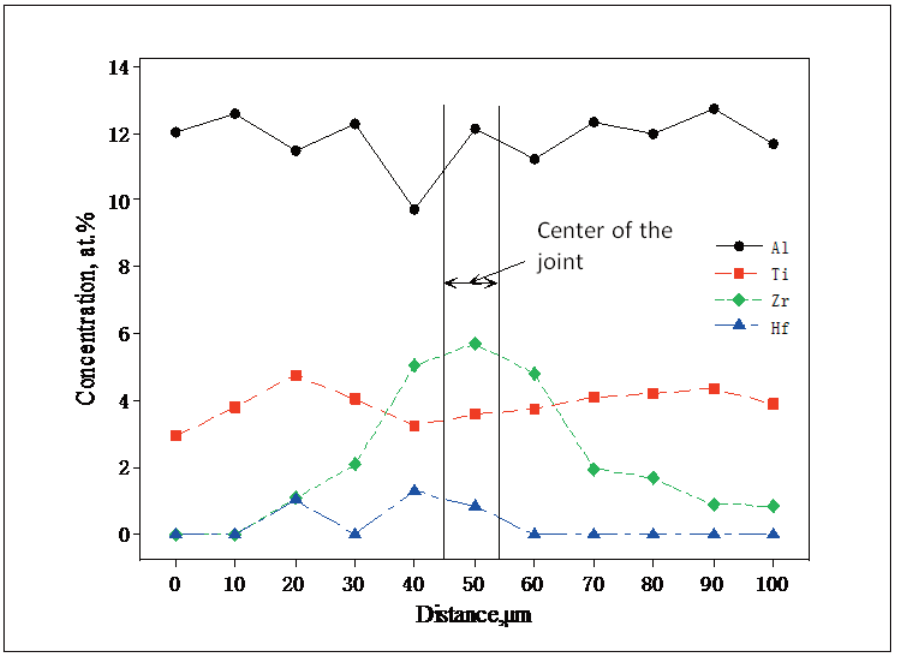

Fig. 8 — Elemental distribution across the braze joint (NGB1).

Results

Visual inspection was conducted after the completion of three brazing cycles. Indication of the brazing alloy was observed around the joint periphery of all samples, suggesting sufficient flow of the alloy during brazing (the brazing alloy foil accounts for only one-fourth of the total mating surface area of the single-crystal bar). In separate WGB trials utilizing the infiltration method (brazing alloy placed on top of filler powder paste), the brazing alloy had penetrated the entire depth of a 7-mm joint clearance (Ref. 25), further confirming the flowability of this alloy.

Microstructure of the Brazing Alloy

The microstructure of the as-cast brazing alloy is shown in Fig. 4. It contains a network of eutectic phases in a γ-Ni matrix.

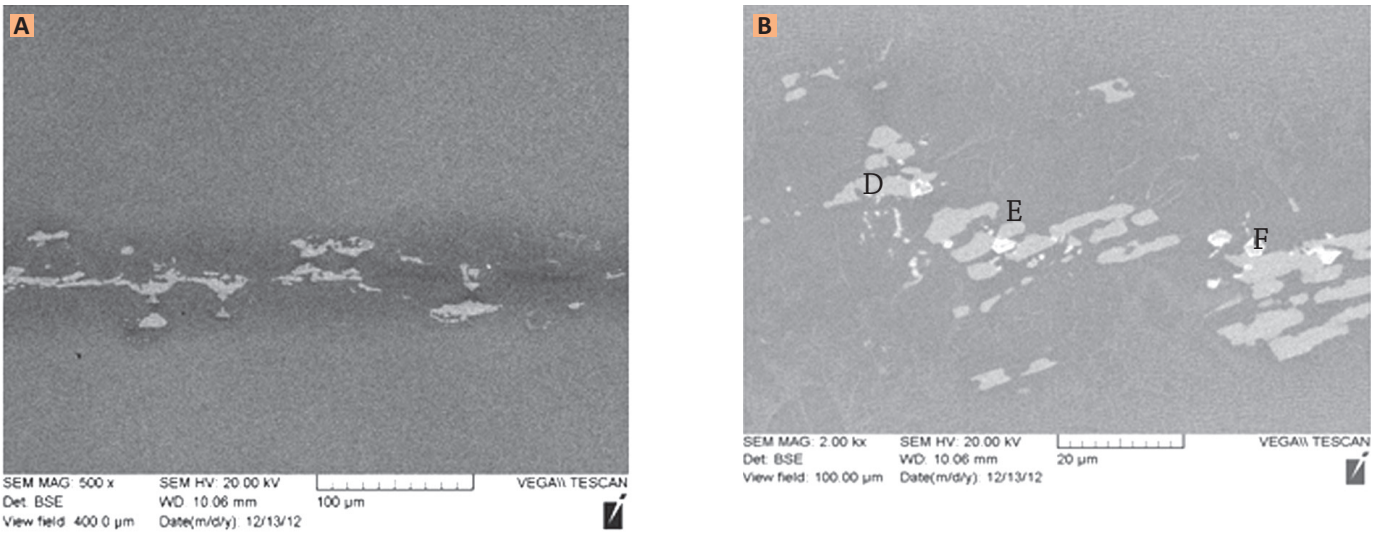

Fig. 9 — SEM images of NGB2 in the as-polished condition. A — low magnification of the joint interface; B — high-magnification micrograph showing three different phases labeled D, E, and F.

Table 5 — Microhardness of Different Phases in the NGB Joint (Refs. 1–3)

NGB1		NGB2		NGB3	
A	B	D	E	G	Eutectic Boride Containing Phases
327 HV	375 HV	329 HV	340 HV	334 HV	720

Microstructure of NGB1

The as-brazed NGB1 in the as-polished condition exhibits a layer of interface containing two noticeable phases (A and C as labeled in Fig. 5B and C). In the substrate CMSX-4, no dendritic structure was observed, likely due to the complete solution treatment carried out at that supplier's facility. The interface is about 100 µm thick, including a band on either side with a darker contrast. The nature of the phases in the interface was further analyzed using EDS with the results, in at.-%, summarized in Table 4. The light phase (A) is more enriched in Zr and Hf, as compared to the surrounding matrix (B), but lacks W, Ti, and Al. The cubic-shaped intermetallic phase (C) contains elevated amounts of Zr, Hf, W, and Re and reduced amount of Ni. Further evaluation of the interfacial structure was conducted under the etched condition with images illustrated in Figs. 6 and 7. A complex microstructure was formed during the NGB process. The interface has predominantly Zr enrichment as seen from X-ray maps — Fig. 7. This suggests that a homogenization heat treatment is required in order to create more uniform microstructure after the initial brazing cycle. The microhardness test, however, revealed that the hardness values of the two Zr-rich phases (A and C) were similar to the surrounding gray matrix phase (B) (Table 5) and much lower than that measured on borides or silicides (Refs. 2, 24). Semiquantitative elemental analysis was also conducted to determine Hf, Zr, Al, and Ti distribution across the interface — Fig. 8. Similarly, the analysis confirmed that Zr was the only element that exhibited nonuniform distribution after the short brazing cycle.

Microstructure of NGB2

Using the same brazing cycle parameters as NGB1 but with the addition of 50 lb/in.^{2} pressure, the NGB joint had much less intermetallic phases. Also, these intermetallic phases became more intermittent with an occasional intermetallic phase-free zone — Fig. 9. Comparing Figs. 5 and 9, the amount of intermetallic phases in the interface region decreased by at least 50%. On the remaining intermetallic phases, EDS analysis (Table 6) was carried out to discern the nature of these phases. Similar to that observed in sample NGB1, the irregular-shaped light phase (D) had increased Zr content while the cubic-shaped phase (F) had elevated amounts of Zr, Hf, and Ta compared to the surrounding region E. X-ray mapping was also conducted to identify elemental distribution. As illustrated in Fig. 10, only Zr is seen to be concentrated in the joint interface region. The EDS line scan analysis results in Fig. 11 also reveal higher Zr content in the joint region; however, the percentage of Zr is slightly less than that in sample NGB1. Additionally, Hf from the brazing alloy has diffused away from the interface, reaching a uniform distribution. It is believed that the ele-

Table 6 — EDS Results of Various Phases in Sample NGB2

Element	Concentration, at.-%		
	D	E	F
Al	8.20	12.60	8.11
Ti	2.08	4.43	3.48
Cr	5.66	5.64	6.47
Co	10.75	10.34	9.26
Ni	59.87	63.67	52.54
Zr	6.57	0.00	9.67
Hf	2.53	0.00	5.84
Ta	1.83	1.78	4.63
W	1.36	1.55	0.00
Re	1.14	0.00	0.00

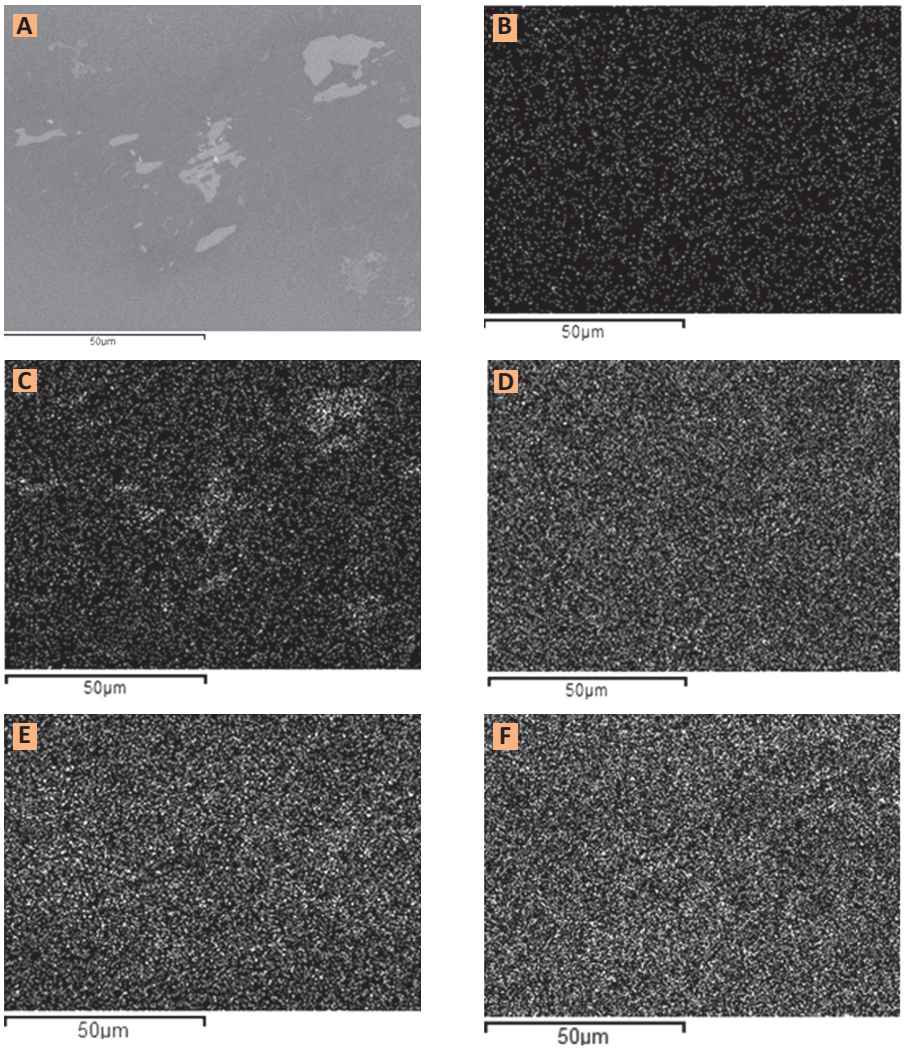

Fig. 10 — Elemental maps (NGB2). A — BSE SEM image; B — Hf; C — Zr; D — Al; E — Ti; F — Cr.

Table 7 — EDS Results for Phases in Sample NGB3

Element	Concentration, at.-%		
	I	G	H
Al	12.82	14.51	9.76
Ti	1.25	2.09	1.13
Cr	8.65	5.61	5.49
Co	11.30	9.50	9.87
Ni	62.39	64.10	63.44
Zr	0.00	0.00	8.20
Hf	0.00	0.00	0.00
Ta	1.57	2.29	0.00
W	2.02	1.90	0.00
Re	0.00	0.00	0.00
Re			2.11

vated Zr content in the joint is due to the formation of Zr-rich intermetallic phases. The dissociation of these will have to take place before diffusion of Zr can occur.

Table 8 — Volume Percentage of Zr-Containing Phase in Three NGB Joints

Volume Percentage of Zr-Rich Intermetallic Phases		
NGB1	NGB2	NGB3
20.1	6.6	0.76

The hardness values at locations D and E are given in Table 5. Similarly, even with the presence of intermetallic compounds, the hardness is quite low compared to a conventionally brazed joint with B or Si.

Sample NGB2 was subsequently etched to reveal the microstructure of the joint and substrate after a brazing cycle at 1240°C for 40 min. The interface still had some remaining intermetallic phases from the use of the brazing alloy. However, the two

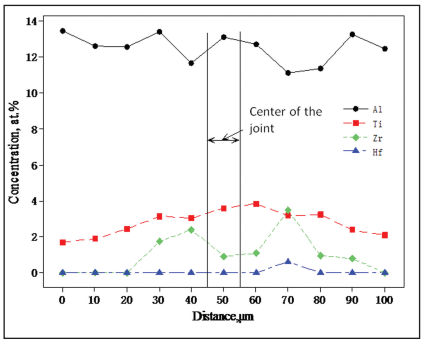

Fig. 11 — Elemental distribution across the braze joint (NGB2).

CMSX-4 buttons were completly joined with no interfacial delamination or voids — Fig. 12A. Also observed was the formation of fine, irregular γ′ on the substrate side of the joint due to the furnace cooling from brazing cycle, as shown in Fig. 12B. There is also an indication of eutectic γ/γ′ formation in the joint — Fig. 12C. To further examine the secondary orientation alignment after the brazing cycle, a separate sample set was brazed at the same temperature and pressure but for a longer duration (24 h) to further remove the intermetallic phases. As shown in Fig. 13, the alignment of secondary orientation between the two CMSX-4 buttons can be seen by observing the cuboidal γ′phases — Fig. 13.

Microstructure of NGB3

With the addition of a homogenization treatment (from NGB1 to NGB3), the interfacial intermetallic phases reduced substantially. In fact, some of the joint region is indistinguishable from the original substrate — Fig. 14A. This suggests that the homogenization treatment is effective in removing the Zr-rich intermetallic phases. The few remaining phases in the joint were further evaluated. As shown in Fig. 14B, microstructure in this area contains a few light particles (H) and a large eutectic region (G), often termed cellular eutectic γ/γ′ in the literature, although strictly speaking, the formation of the cellular region is through a peritectic reaction (Ref. 26). From the EDS compositional analysis (Table 7), region G is found to have essentially Ni (Cr and Co) and Al. The light phase

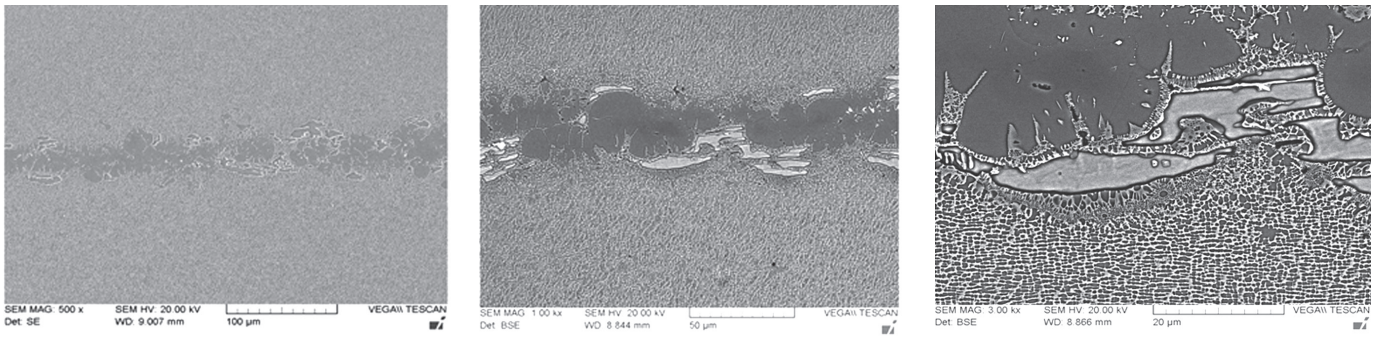

Fig. 12 — SEM images after etching (NGB2).

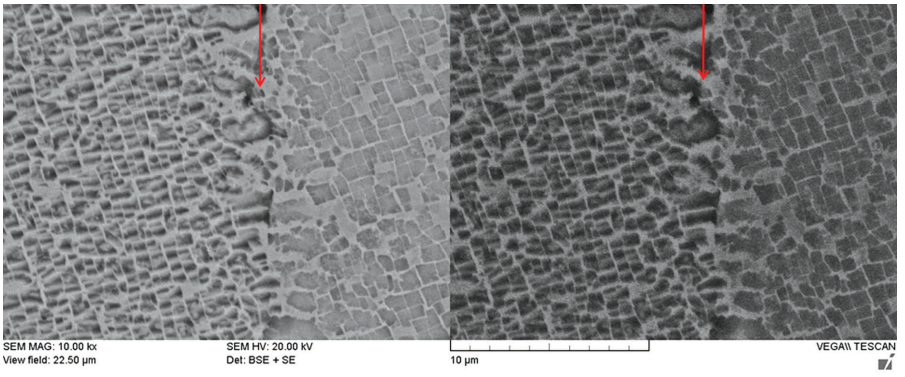

Fig. 13 — SEM images showing the alignment of secondary orientation using pre-scribed indexing line (1240°C for 24 h, arrows point to the interface).

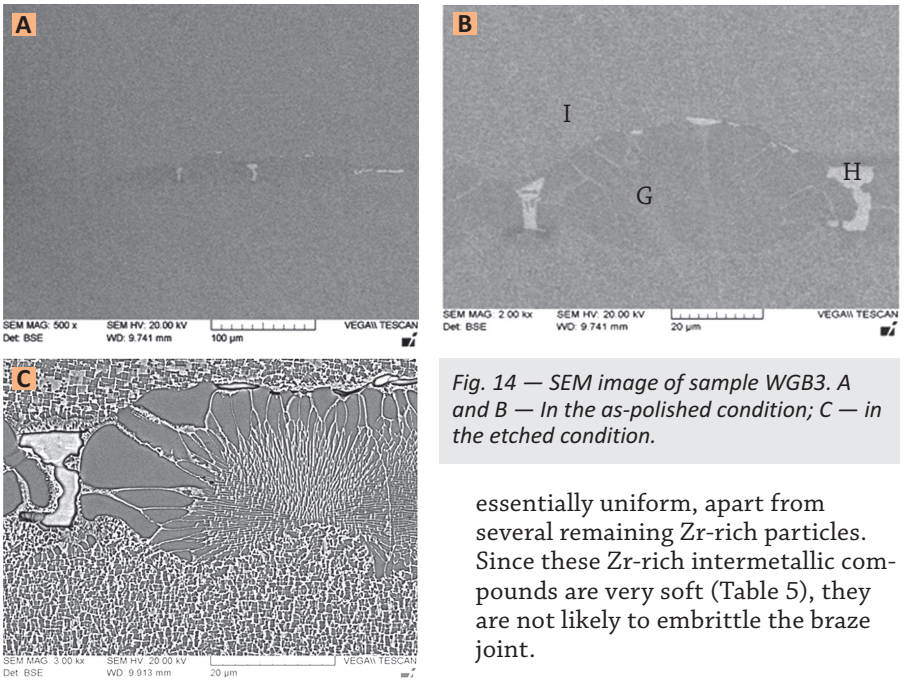

Fig. 14 — SEM image of sample WGB3. A and B — In the as-polished condition; C — in the etched condition.

H (Fig. 14B) is a Zr-rich intermetallic compound that has not been removed during the homogenization treatment. Comparing Figs. 8 and 15, the composition across the joint after 10 h of homogenization treatment is essentially uniform, apart from several remaining Zr-rich particles. Since these Zr-rich intermetallic compounds are very soft (Table 5), they are not likely to embrittle the braze joint.

Discussion

In this study, three different brazing processes were employed to join SX CMSX-4 using boron- and silicon-free brazing alloy. The brazing temperature of 1240°C was found suitable to join CMSX-4 without apparent interfacial defects. Although all three joints contained Zr-rich intermetallic compounds, the total volume percentage was reduced by the application of pressure or homogenization heat treatment at 1200°C for 10 h. Table 8 shows the volume percentages of intermetallic compounds within a band of 75 µm in width along the interface. Comparing NGB1 and NGB2 to that produced by other researchers (Ref. 6) using similar brazing temperature but a longer cycle (Fig. 16), it is found the intermetallic compounds in NGB1 and NGB2 are substantially less evident.

The effects of the pressure application for braze joints have been examined by many researchers (Refs.16, 27–29). When being applied adequately (not to the extent of displacing the brazing alloy excessively from the joint or deform the joints), it has the advantages to decrease the amounts of intermetallic compounds, increase joint strength and ductility, improve interfacial bonding, and the potential to reduce the brazing temperature and time. An "ejection model" was used to explain the improved joint microstructure and mechanical properties when brazed with MBF (Metglas™ brazing foil) (Ref. 30). It's essentially a mechanical redistribution of the liquid metal (enriched in MPD, and hence, intermetallic compound upon solidification) first formed during brazing. This in turn reduces the amount of intermetalllic phases formed in the solidified joint. Combining the application of pressure and homogenization heat

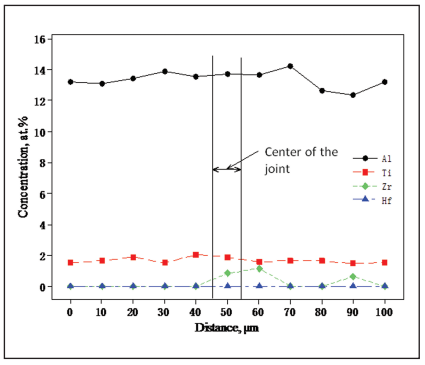

Fig. 15 — Elemental distribution of Al, Ti, Zr, and Hf after homogenization treatment (NGB3).

treatment, the intermetallic-containing layer will be reduced further, likely leaving behind a homogeneous joint microstructure.

It was also observed that the diffusion of Hf out of the joint occurred more readily (than Zr) after the initial brazing cycle. And diffusion of Zr also ensued rapidly after homogenization heat treatment. Another factor that needs to be taken into consideration during repair of turbine components is the residual stress on the serviced parts. Stressed materials, particularly single-crystal superalloys, will likely develop localized cellular transformation γ/γ' structure upon being heated (such as that during brazing cycle) (Ref. 21). If it is not completely removed through heat treatment, the presence of cellular structure is detrimental to the mechanical properties of the components. During braze repair, if grain boundary strengtheners (B, Zr, and Hf) can be incorporated into the joint, they can alleviate the damaging effect. In this study, cellular γ'/γ' structure was observed in all three joints. While there have been reports on the reduced fatigue life in the presence of cellular structure, the presence of Zr and Hf in the joint, particularly along the cellular boundaries, will be beneficial in ensuring that the detrimental effect of cellular structure can be minimized. Additionally, since a furnace cooling was employed in this study, the size of cellular γ'/γ' structure was relatively large due to the slow cooling rate. If the cooling rate can be increased by using an Ar quench, for example, the cellular γ'/γ' structure will likely be much smaller (Ref. 31).

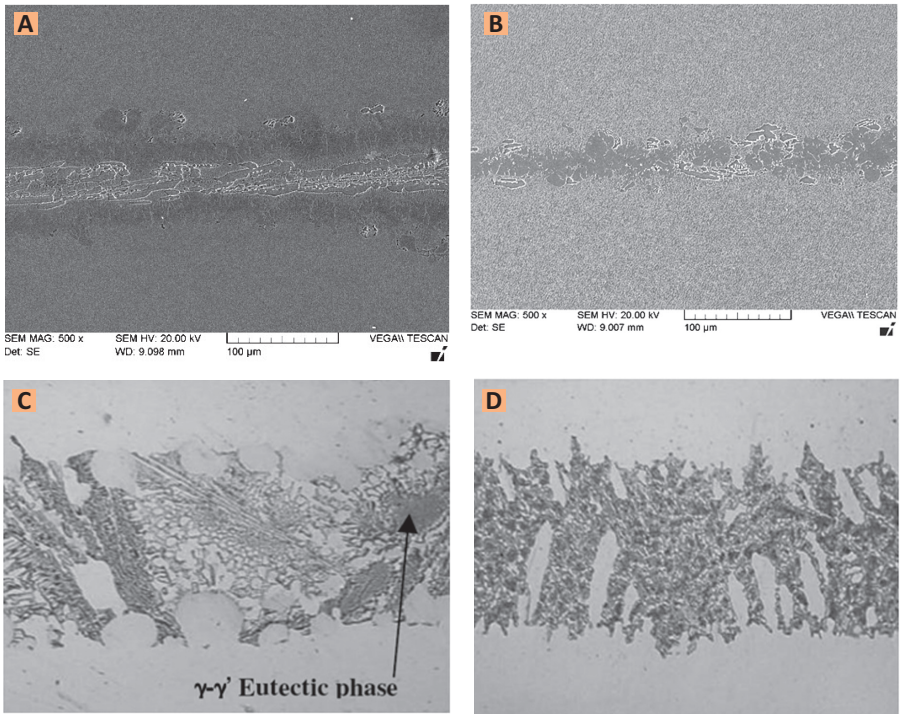

Fig. 16 — Comparison of NGB joints with that from literature. A — NGB1 and B — NGB2 joints produced in this study without the application of pressure; C — NGB joint with hypereutectic Ni-Cr-Hf alloy, 1238°C/18 h (200×) (Ref. 6); D — NGB joint with hypereutectic Ni-Cr-Zr, 1238°C/18 h (200×) (Ref. 6).

Conclusions and Future Work

In this study, a new boron- and silicon-free brazing alloy based on Ni-Co-Zr-Hf-Cr-Ti-Al was developed and used to join CMSX-4 single-crystal superalloy under three conditions. It was found that using a combination of Hf and Zr as a melting point depressant, in addition to other elements, both elements in the initial brazing alloy can be effectively reduced while still achieving a relatively low liquidus. The new alloy successfully joined CMSX-4 with complete metallic bonding, under all three conditions. Although two types of interfacial Zr-rich intermetallic compounds were observed after 40 min of brazing cycle, their hardness values were similar to that of the superalloy substrate. Furthermore, with the application of pressure during brazing or postbrazing homogenization heat treatment, the intermetallic compounds were substantially reduced.

Future work will focus on testing of joint mechanical properties (high-temperature tensile, LCF, and creep) in addition to joint coatability/coating-joint interaction, since nowadays most of the refurbished turbine components are coated before being returned to service.

Acknowledgments

The author would like to thank Carleton University for the Research Award to support this work. The help from Dr. F. Gao for sample preparation and SEM imaging is greatly appreciated.

References

1. American Welding Society. 1991. *Brazing Handbook*, 4th ed.

2. Huang, X., and Miglieti, W. 2011. Wide gap braze repair — a review. *Journal of Engineering of Gas Turbine and Power* 134(10): 010801.

3. Schoonbaert, S., Huang, X., Yandt, S., and Au, P. 2008. Brazing and wide gap repair of X-40 with IN 738. *Journal of Engineering for Gas Turbines and Power* 130(3): 32101–32110.

4. Henhoeffer, T., Huang, X., Yandt, S., and Au, P. 2011. Fatigue properties of narrow and wide gap braze repaired joints. *Journal of Engineering for Gas Turbines and Power* 133(9): 92101.

5. Henhoeffer, T., Huang, X., Yandt, Seo, D., and Au, P. 2009. Microstructure and high temperature tensile properties of narrow gap braze joint between X-40 and IN738. *Journal of Material Science and Technology* 25(7): 840–850.

6. Miglietti, W., and Toit, M. 2008. High strength, ductile braze repair for stationary gas turbine components — Part 1. *ASME Turbo Expo 2008: Power for Land, Sea and Air*, Berlin, Germany, GT2008-51133.

7. Miglietti, W., and Toit, M. 2009. High strength, ductile braze repair for stationary gas turbine components — Part 2. *ASME Turbo Expo 2009: Power for Land, Sea and Air*, Orlando, Fla., GT2009-60210.

8. Buschke, I., and Lugscheider, E. 1998. New approaches for joining high-temperature materials. *Proceedings from Materials Conference '98 on Joining of Advanced and Specialty Materials*, Ill., pp. 57–62.

9. Humm, S., and Lugscheide, E. 2001. Investigations of the chemical and the mechanical-technological behavior of chromium bearing Ni-Hf filler metals. *Proceedings from Joining of Advanced and Specialty Materials*, Indianapolis, Ind., ASM International, pp. 39–43.

10. Zheng, Y., Ruan, Z., and Zheng, Y. 1990. Microstructure and performance of Ni-Hf brazing filler alloy. *Acta Metall Sinica* 26(2): 125–131.

11. Miglieti, W. 2003. Diffusion bonding of gaps, U.S. patent 6,520,401.

12. Laux, B., Piegert, S., and Rosler, J. 2008. Fast epitaxial high temperature brazing of single crystalline nickel based superalloys. *ASME Turbo Expo 2008: Power for Land, Sea and Air*, Berlin, Germany, paper GT2008-50055.

13. Laux, B., Piegert, S., and Rosler, J. 2008. Advancements in fast epitaxial high temperature brazing of single crystalline nickel based superalloys. *ASME Turbo Expo 2009: Power for Land, Sea and Air*, Orlando, Fla., paper GT2009-59264.

14. Dinkel, M., Heinz, P., Pyczak, F., Volek, A., Ott, M., Affeldt, E., Vossberg, A., Goken, M., and Singer, R. F. 2008. New boron and silicon free single crystal diffusion brazing alloys. *Superalloys 2008,* TMS, pp. 211–220.

15. Neumeier, S., Dinkel, M., Pyczak, F., and Goeken, M. 2000. Nanoindentation and XRD investigation of single crystalline Ni-Ge brazed nickel-based superalloys PWA 1483 and Rene N5. *Materials Science and Engineering* A 528(3): 815–822.

16. Rabinkin, A. 2010. High temperature brazing development since the time of the "bow-tie generation": in memory of Robert L. Peaslee. *LOT 2010,* Aachen, Germany, Brazing, high temperature brazing and diffusion bonding, pp. 1–8.

17. Zheng, Y., Zhao, L., and Tangri, K. 1993. Microstructure of Ni-10Co-8Cr-4W-13Zr alloy and its bonding behaviour for single-crystal nickel-base superalloys. *Journal of Materials Science* 28: 823–829.

18. Budinger, D., Ferrigno, S., and Murphy, W. 1993. Alloy powder mixture for brazing of superalloy articles, U.S. patent 5,240,491,1993.

19. Wilson, B., Hickman, J., and Fuchs, G. 2003. The effect of solution heat treatment on a single crystal Ni-based superalloy. *J. of Metals* (3): 35–40.

20. Meng, J., Jin, T., Sun, X., and Hu, Z. 2011. Surface recrystallization of a single crystal nickel-base superalloy. *International Journal of Minerals, Metallurgy and Materials* 18(2): 197–202.

21. Okazaki, M., Ohtera, I., Harada, Y., and Namba, K. 2003. Undesirable effect of local cellular transformation in microstructurally controlled Ni-base superalloys subjected to previous damage on high temperature fatigue strength and the prevention: for recoating and refurbishment technology. *Mater. Sci. Res. Int*. 9(1): 55–60.

22. Okazaki, M., Ohtera, I., and Harada, Y. 2004. Damage repair in CMSX-4 alloy without fatigue life reduction penalty. *Met. Trans.* 35A(2): 535–542.

23. Zambaldi, C., Roters, F., Raabe, D., and Glatzel, U. 2007. Modeling and experiments on the indentation deformation and recrystallization of a single-crystal nickel-based superalloy. *Mat. Sci. and Eng.* A 454-45, pp. 433–440.

24. Okazaki, M., Hiura, T., and Suzuki, T. 2000. Effect of local cellular transformation on fatigue small crack growth in CMSX-4 and CMSX-2 at high temperature. *Reburbishment Technology, Superalloys 2000*, TMS, Warrendale, pp. 505–514.

25. Huang, X. 2014. Wide gap brazing of IN 738 with boron-free Ni-Cr-Zr-Hf-Cr-Ti-Al braze alloy. *ASME Turbo Expo 2014: Turbine Technical Conference and Exposition*. Dusseldorf, Germany, paper GT2014-250025.

26. Warnken, N., Ma, D., Mathes, M., and Steinbach, I. 2005. Investigation of eutectic island formation in SX superalloys. *Mat. Sci. and Eng*., A413-414, pp. 267–271.

27. Yeh, M. S., and Chuang, T. H. 1997. Effects of applied pressure on the brazing of superplastic Inconel 718 superalloy. *Metallurgical and Materials Transactions* A 28(6): 1367–1376.

28. Moore, T. J. Preliminary study on the pressure brazing and diffusion welding of Nb-1Zr to Inconel 718. *Welding Journal* 69(3): 98-s to 102-s.

29. Brazing and Soldering. 2007. *Proceedings of the 3rd International Brazing and Soldering Conference*, ed. J. J. Stephens and K. S. Weil, American Welding Society, San Antonio, Tex.

30. Rabinkin, A., and Pounds, S. 1988. Effects of load on brazing with METGLAS® MBF-2005 filler metal. *Welding Journal* 67(5): 33–43.

31. Seo, S. M., Lee, J. H., Yoo, Y. S., Jo, C. Y., Miyahara, H., and Ogi, K. 2011. A comparative study of the γ/γ' eutectic evolution during the solidification of Ni-base superalloys. *Met. Trans.* 42A(10): 3150–3159.